

Third-order Electrical Conductivity of the Charge-ordered Organic Salt α -(BEDT-TTF)₂I₃

Mayu Ishii, Ryuji Okazaki,* and Masafumi Tamura

Department of Physics, Faculty of Science and Technology, Tokyo University of Science, Noda 278-8510, Japan

We performed third-order electrical conductivity measurements on the organic conductor α -(BEDT-TTF)₂I₃ using an ac bridge technique sensitive to nonlinear signals. Third-order conductance G_3 is clearly observed even at low electric fields, and interestingly, G_3 is critically enhanced above the charge-order transition temperature $T_{CO} = 136$ K. The observed frequency dependence of G_3 is incompatible with a percolation model, in which a Joule heating in a random resistor network is relevant to the nonlinear conduction. We instead argue the nonlinearity of the relaxation time according to a phenomenological model on the mobility in materials with large dielectric constants, and find that the third-order conductance G_3 corresponds to the third-order electric susceptibility χ_3 . Since the nonlinear susceptibility is known as a probe for higher-order multipole ordering, the present observation of the divergent behavior of G_3 above T_{CO} reveals an underlying quadrupole instability at the charge-order transition of the organic system.

Electronic crystallization on a lattice, known as charge ordering, is an emergent phenomenon driven by strong electron-electron interactions [1–4]. It is well materialized in a class of organic molecular conductors, and a quasi-two-dimensional (quasi-2D) charge transfer salt α -(ET)₂I₃ [ET being bis(ethylenedithio)-tetrathiafulvalene (BEDT-TTF)] is known as a quite essential material to show charge ordering. α -(ET)₂I₃ exhibits a metal-insulator transition at $T_{CO} = 136$ K [5], below which a stripe-type charge disproportionation (charge ordering) has been observed by various experimental methods including nuclear magnetic resonance [6, 7], optical measurements [8–13], and synchrotron radiation x-ray diffraction [14]. An electronic ferroelectricity without inversion symmetry is detected by second harmonic generation technique [15] and the polarization switching is also confirmed [16]. Interestingly, this charge-ordered state is highly sensitive to the external perturbations to realize massless Dirac fermions in hydrostatic pressure and superconducting state under uniaxial pressure [17–20].

Among the various intriguing properties of α -(ET)₂I₃, the detailed response function for the electric field, which may act as a conjugate field to the electronic crystal, is of fundamental interest. Indeed, charge ordering in α -(ET)₂I₃ shows non-trivial behavior for applied electric field [21–31], and moreover, a novel current-induced thermoelectric phenomenon has been also suggested recently [32, 33]. Dressel *et al.* first reported a nonlinear electrical conductivity above the threshold fields [21], reminiscent of sliding motion of charge density wave (CDW). Voltage oscillation and Shapiro steps have been subsequently observed above the threshold fields [22, 23], indicating a collective excitation of charge ordering similar to CDW [24]. In addition, nonequilibrium hot-electron state is recently proposed by simultaneous optical and transport measurements at high fields [25], while a scanning Raman microspectroscopy experiment has clearly shown that application of such a high electric field triggers a filamentary-like spatially-inhomogeneous state [26], which often becomes an extrinsic origin of nonlinear conduction [34]. At low fields where such a spatial inhomogeneity is irrelevant, a nonlin-

ear conduction is also examined and the observed power-law current(I)-voltage(V) curves ($I \propto V^\alpha$) are explained by thermal excitation of electron-hole pairs from 2D logarithmic potential [27]. In particular, the power-law exponent α in low-field range abruptly changes from $\alpha = 1$ to 3 below $T_{KT} \approx 35$ K, suggesting an occurrence of a Kosterlitz-Thouless transition at T_{KT} [28]. In contrast, above T_{KT} , an Ohmic I - V curve ($\alpha = 1$) is obtained at low fields even in the charge-ordered phase; a crucial issue how the nonlinear response emerges with the formation of the charge ordering at T_{CO} has not been discussed.

The aim of this paper is to clarify such an unexplored relation in α -(ET)₂I₃ by means of the third-order electrical conductivity measurements. This harmonic method enables us to directly measure the nonlinear conductivity in low-field range by detecting 3ω component for the applied voltage with a fundamental frequency ω , in contrast to conventional pulsed technique in which the self-heating effect is unavoidable at high fields. The third-order conductance G_3 has been observed in a whole temperature range across T_{CO} and largely enhanced at T_{CO} . To explain this nonlinearity, we refer to the mobility of the polar materials recently investigated, and find that the third-order conductance G_3 approximately corresponds to the third-order electric susceptibility χ_3 , which expresses a quadrupole fluctuation. Our present results thus imply a quadrupole nature in the charge-ordered organic salt α -(ET)₂I₃.

Single crystals of α -(ET)₂I₃ were prepared by an electrochemical method. Two gold wires were attached by using a gold paste to reduce the contact resistance [35] and the voltage was applied along the in-plane direction. The rate of temperature change is lower than 0.3 K/min to prevent the damage to the sample. As schematically shown in the inset of Fig. 1(a), third-order electrical conductivity measurements were performed by using a bridge circuit to exclude the extrinsic third-order terms coming from nonlinearities of voltage source and electrical circuit inside the lock-in amplifier [36–38]. When a sample exhibits nonlinear conductivity, electrical current I flowing in the sample under the applied voltage V_s , is expressed by a Taylor series as

$$I \simeq I_1 + I_3 = G_1 V_s + G_3 V_s^3, \quad (1)$$

where I_1 (G_1) and I_3 (G_3) are linear and third-order current

* okazaki@rs.tus.ac.jp

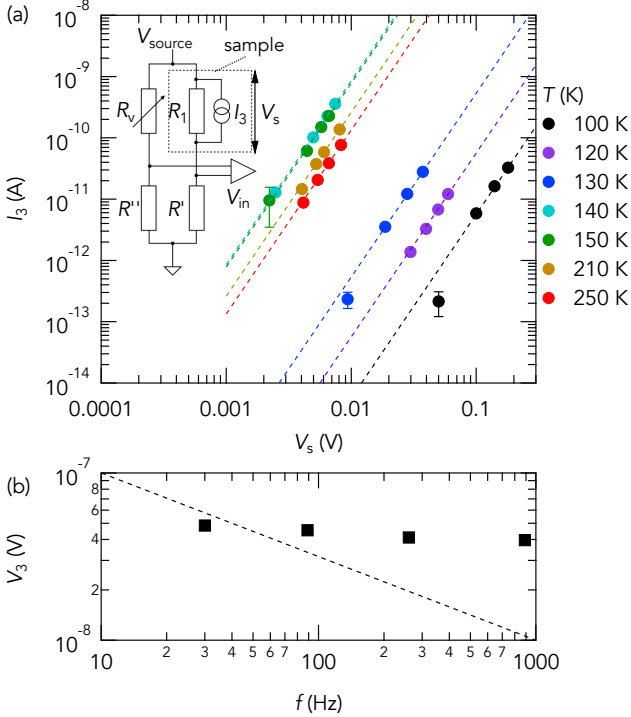


FIG. 1. (Color online) (a) In-phase components of third-harmonic current I_3 as a function of the applied voltage to the sample V_s measured at several temperatures. The dashed lines represent the V_s^3 dependence. The inset depicts the bridge circuit to exclude the linear voltage into the lock-in amplifier. (b) The frequency dependence of the third-harmonic voltage V_3 measured at $T = 136$ K with the sample voltage of $V_s \approx 6$ mV. The dashed lines represent the $f^{-1/2}$ dependence, which is expected in the case that the self-heating effect is dominant.

(conductance), respectively [38], and the higher-order terms are assumed to be negligible. Note that the inversion symmetry is broken below T_{CO} in α -(ET) $_2$ I_3 but we have not applied a magnetic field in this experiment, so the second-order term $G_2 V_s^2$ is not considered here [39]. Thus, the sample can be regarded as a parallel circuit consisting of a linear resistance $R_1 = G_1^{-1}$ and a nonlinear current source I_3 .

In the bridge circuit, the input voltage to the lock-in amplifier V_{in} is then given as

$$V_{in} = \frac{R_1 R'' - R_v R'}{(R_1 + R')(R_v + R'')} V_{source} - \frac{I_3}{1/R_1 + 1/R'}, \quad (2)$$

where R_v , R' , and R'' are resistances constituting the bridge circuit and V_{source} is the source voltage [38]. The voltage signal measured by a lock-in amplifier V_m must contain small but finite nonlinear components as $V_m \approx V_{in} \{1 + \beta(V_{in})\}$, where non-dimensional $\beta(V_{in})$ is a series of V_{in} to express the nonlinearity in the lock-in amplifier, order of which is typically 10^{-4} [38]. Here, in the balanced condition of $R_1 R'' = R_v R'$, the first term in the right-hand side of Eq. (2) becomes zero, and then the nonlinearity of the voltage source can be excluded.

In addition, in the balanced condition, one can also eliminate the nonlinearity of the lock-in amplifier since the third-order term, $-I_3/(1/R_1 + 1/R')$, becomes the leading term. Moreover, in the measured frequency range, the frequency dependence of the linear conductivity is negligible, i.e. $G_1(\omega) = G_1(3\omega)$ [16], so that the balanced condition is kept both in ω and 3ω . Note that this harmonic technique is similar to the 3ω method for thermal conductivity measurements [40, 41] and the ac method for the specific heat measurements [42, 43], in which the harmonic signals from the heater and the thermometer are respectively measured, while the present method detects the third-harmonic voltage of the sample directly.

In this experiments, we applied the ac voltage $V_{source}(t) = V_0 \sin \omega t$ to the circuit with the frequency of $f = \omega/2\pi = 89$ Hz, and measured the fundamental voltage V_1 and the third-harmonic voltage V_3 simultaneously as $V_m = V_1 \sin \omega t + V_3 \sin 3\omega t$ by using two lock-in amplifiers to detect 1ω and 3ω signals. We then balance the circuit by adjusting variable resistance R_v to achieve $V_1 = 0$, and obtain I_3 by using measured V_3 as

$$I_3 = -(1/R_1 + 1/R')V_3 = G_3 V_s^3, \quad (3)$$

where $V_s \approx V_0 R_1 / (R_1 + R')$ is the applied voltage to the sample [38]. It is worth to note that the measured voltage ratio V_3/V_1 is as small as the order of 10^{-6} , which demonstrates the necessity of the bridge technique to exclude extrinsic nonlinearities as mentioned above. We also utilized a four-terminal double-bridge method [37] for the low-resistance range and the results were similar to that of the two-terminal bridge method.

Figure 1(a) depicts the in-phase component of the third-harmonic current I_3 as a function of V_s obtained at several temperatures. Hereafter all the current and voltage data are expressed by rms. Although the signals are comparable to the noise level at the low-current range below 10^{-12} A, which is close to the noise level in the earlier report [28], I_3 is certainly proportional to V_s^3 , and the slope gives the third-order conductance G_3 according to Eq. (3). We emphasize that the electric field corresponding the present voltage is lower than 10 V/cm at $T = 100$ K, which is fairly low compared with the earlier reports [22, 23, 25].

Figure 2(a) compares temperature dependence of the fundamental and third-order conductances G_1 and G_3 , both of which are the in-phase components. Note that, although we utilize the two-terminal method owing to the usage of bridge circuit, the obtained temperature variation of $\sigma_1 = G_1 \times (L/S)$, where $L \approx 4 \times 10^{-2}$ cm and $S \approx 1 \times 10^{-5}$ cm 2 are the length between the terminals and the cross-sectional area respectively, is close to that measured by the four-terminal method, implying that the effect of the contact resistance formed by the gold paint is negligible. Figures 2(b) and 2(c) represent the temperature variations of the in-phase and out-of-phase components of third-order conductance G_3 , respectively. Interestingly, G_3 is observed even above $T_{CO} = 136$ K, and compared with temperature dependence of G_1 , $G_3(T)$ is notably enhanced near T_{CO} , as is discussed in the following section.

Let us consider the origin of the observed third-order nonlinearity. Although there are various causes of the nonlinear conduction, as categorized in Table I, one may first sort

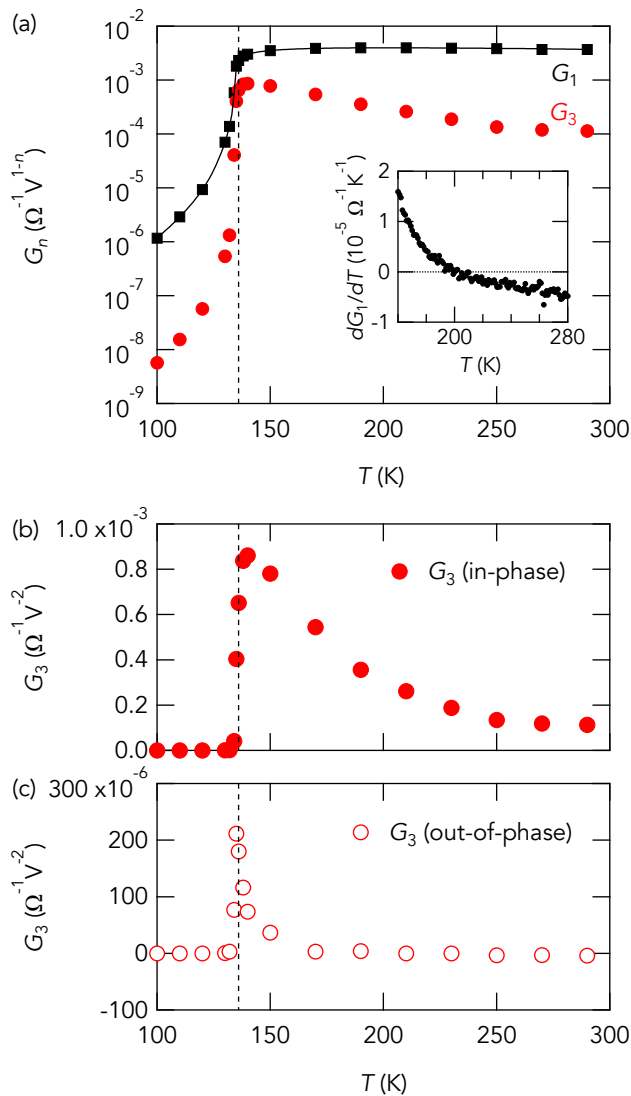


FIG. 2. (Color online) (a) Temperature variations of the linear conductance G_1 (squares) and the in-phase component of the third-harmonic conductance G_3 (circles). Solid curve is the linear conductance measured with a constant current of $I = 10$ nA. The inset shows temperature dependence of dG_1/dT . (b,c) In-phase and out-of-phase components of the third-harmonic conductance G_3 as a function of temperature. Dashed line represents the charge order transition temperature $T_{CO} = 136$ K.

it whether the conductivity σ varies when the temperature changes. Note that the applied electric field to the sample is lower than the threshold field [22, 23], above which charge ordering shows a collective sliding mode as is similar to that of CDW [44]. It should also be emphasized that there are few studies on the third-harmonic conductivity [45, 46] and the interpretation remains unclear. In the simplest case, the phonon (lattice) temperature T_p increases to $T_p + \Delta T_p$ by the applied power of $G_1 V^2$, and then the conductivity seems to be varied, which is well known as the extrinsic self-heating effect. In this case, the conductance is expressed as $G(V) \approx$

$G_1 + (\partial G_1 / \partial T_p) \Delta T_p$ and the temperature increase is given as $\Delta T_p = R_{th} G_1 V^2$, where R_{th} is the thermal resistance between the sample and the thermal bath, leading to the third-order conductance of $G_3 = R_{th} G_1 (\partial G_1 / \partial T_p)$ [37]. This heating effect is unlikely in the present case, because the sign of observed G_3 is positive while $\partial G_1 / \partial T_p$ changes its sign at around 200 K as seen in the inset of Fig. 2(a). Note that this non-linearity due to the heating effect is of importance to detect higher-order moment of the current distribution in the percolation network consisting of the metallic and insulating domains in the sample. In this case, a peculiar frequency dependence of $V_3 \propto f^{-1/2}$ is expected [37]. On the other hand, the observed V_3 shows almost no frequency dependence as shown in Fig. 1(b), again indicating that the heating effect is unlikely in the present case.

We then discuss the hot-electron model. In this scenario, an electron temperature T_e , which is larger than T_p , is enhanced by applying electric field to vary the conductivity. This model is suggested to explain the high-field nonlinearity in this material [25]. In this case, the electron and phonon systems are connected with the thermal resistance R_{ep} and the characteristic time scale τ_e is given as $\tau_e = R_{ep} C_e$, where C_e is the electronic specific heat [47]. Now the order of τ_e is generally as small as 10^{-9} s, and thus previous hot-electron phenomena have been investigated by using a pulsed technique with a short pulse width of 10^{-9} s [47]. In contrast, the period of the applied voltage in the present measurement of $f^{-1} \sim 10^{-2}$ s is much longer than τ_e . Therefore, the electron and lattice systems are in equilibrium ($T_e \approx T_p$) in the present time scale, and thus hot-electron scenario is excluded due to the same reason to the self-heating case as discussed above.

Next we argue a non-thermal origin for nonlinear conduction, which is not induced through the temperature change in field. If we adapt a simple Drude formula of $\sigma = en\mu$ for the measured temperature range, where n and μ are the carrier density and the mobility, respectively, one may consider the electric-field dependence of n and/or μ for the nonlinearity of σ . According to Refs. 27 and 28, the charge gap Δ is effectively reduced by the field E as $\Delta(E) = U_0 \ln(\lambda/a) - e\lambda E$, where λ is a cutoff length of the potential and a is the minimum length scale taken as the size of the ET molecule, resulting in increase of the activation-type conductivity $\sigma(E) = \sigma_0 \exp[-\Delta(E)/2k_B T]$ due to the field-induced increase of the carrier density $n(E)$. However, this scenario is based on the 2D logarithmic potential developed well below T_{CO} , in contrast to the present results that the nonlinearity appears critically above T_{CO} .

We then consider possible field-dependent mobility $\mu(E)$.

TABLE I. A simple sort of origins for the nonlinear conduction in low field range.

$\sigma(E)$	$\frac{\sigma[T(E)]}{\sigma(E)}$	$\frac{\sigma[T_p(E)]}{\sigma[T_e(E)]}$	self-heating effect [37]
			hot electron [47]
		$\frac{en(E)\mu}{en\mu(E)}$	field-dependent energy gap [27, 28]
			field-dependent mobility

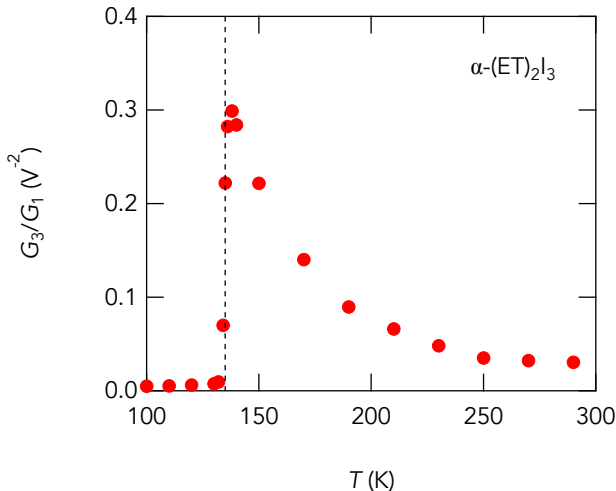


FIG. 3. (Color online) Temperature dependence of the ratio of the in-phase components of G_3 to G_1 . Dashed line represents the charge order transition temperature $T_{CO} = 136$ K.

Recently, it has been suggested that the mobility in the large-permittivity compound is expressed as $\mu \propto \varepsilon^{1/2}$ (ε is the permittivity) [48, 49]. Here, mean free path l in large-permittivity materials may be proportional to the Thomas-Fermi screening length r_{TR} , since it gives a characteristic length scale for the potential modulation which acts as the scattering centers [48]. In such a case, since $r_{TR} \propto \sqrt{a_B^*}$, where a_B^* is the effective Bohr radius given as $a_B^* = (\varepsilon/\varepsilon_0)(m/m^*)a_B$ (ε_0 being the vacuum permittivity, m the electron mass, m^* the effective mass, a_B the Bohr radius), the mobility μ is given as $\mu \propto l \propto \varepsilon^{1/2}$. Here, the permittivity is given as $\varepsilon = \varepsilon_0(1 + \chi)$ and the electric susceptibility χ is generally expanded as $\chi \approx \chi_1 + \chi_3 E^2$, where χ_1 and χ_3 are linear and third-order electric susceptibilities, respectively. Up to the E^2 term, we then obtain a field-dependent mobility as

$$\mu(E) \propto (1 + \chi)^{1/2} \approx (1 + \chi_1)^{1/2} \left(1 + \frac{1}{2} \frac{\chi_3}{1 + \chi_1} E^2 \right). \quad (4)$$

Therefore, by comparing it with $\sigma = en\mu \approx \sigma_1[1 + (\sigma_3/\sigma_1)E^2]$, the conductance ratio is given as

$$\frac{G_3}{G_1} \propto \frac{\sigma_3}{\sigma_1} \propto \frac{1}{2} \frac{\chi_3}{1 + \chi_1}. \quad (5)$$

In Fig. 3, we plot temperature dependence of G_3/G_1 . Interestingly, it exhibits a peak structure near T_{CO} , indicating

an enhancement of the third-order electric susceptibility χ_3 at the charge-order transition. Note that the linear susceptibility χ_1 in the denominator is difficult to contribute to the enhancement of G_3/G_1 , because χ_1 is usually enhanced near the charge-order transition as seen in the one-dimensional organic salts [50] while it is very difficult to measure χ_1 above T_{CO} in α -(ET) $_2$ I $_3$ owing to the high conductivity [51]. We also mention that the observed enhancement of the out-of-phase component of G_3 at T_{CO} [Fig. 2(c)] may support this picture because the imaginary part of the complex conductivity $\tilde{\sigma} = \sigma + i\omega\chi\varepsilon_0$ generally expresses the electric susceptibility.

In general, third-order electric susceptibility thermodynamically represents the fluctuation of the quadrupole moments [52]. In the magnetic analogy, the higher-order magnetic susceptibility is known as the probe for multipole ordering [53, 54]. Therefore, the present results imply a quadrupole instability hidden in the charge-ordered salt α -(ET) $_2$ I $_3$, which may be natural in a sense that it is also an even-ordered multipole expansion. It should be noted that a signature of charge order is observed with an inhomogeneity even in the high-temperature metallic phase [11, 55]. Also note that such a quadrupole nature is mentioned in κ -type ET salt [45] and manganese oxide [46], although these nonlinear experiments were performed with a standard lock-in technique without bridge circuit in contrast to the present study. Now the quadrupole nature in α -(ET) $_2$ I $_3$ may be attributed to two possible origins: Firstly, the charge-density distribution should be asymmetric in the ET molecule, leading to the quadrupole moment. This is supported by the fact that the framework of ET molecule is sensitive to the amount of charge [56]. Note that the precise determination of the molecular structure using the synchrotron radiation is recently developed [57, 58]. Secondly, the charge distribution inside the unit cell becomes more asymmetric by the formation of charge ordering at T_{CO} . This is also deduced from the temperature dependence of the in-plane anisotropy of the resistivity [59, 60]. At present, it is difficult to clarify the most appropriate interpretation; both origins seem to contribute to the quadrupole instability.

To summarize, we have measured the third-order conductivity of α -(ET) $_2$ I $_3$ over a broad temperature range across the charge ordering transition temperature $T_{CO} = 136$ K. We find the enhancement of the third-order conductance at T_{CO} , which may attribute to the possible quadrupole instability hidden in the charge-ordered organic salt.

ACKNOWLEDGMENTS

We thank M. D. Anoop, N. Kikugawa, Y. Maeno, I. Terasaki, K. Ueda, and S. Yonezawa for discussion. This work was supported by JSPS KAKENHI Grants No. 17H06136.

-
- [1] H. Seo, J. Merino, H. Yoshioka, and M. Ogata, *J. Phys. Soc. Jpn.* **75**, 051009 (2006).
 [2] C. Hotta, *Crystals* **2**, 1155 (2012).
 [3] R. T. Clay and S. Mazumdar, *Phys. Rep.* **788**, 1 (2019).

- [4] M. Dressel and S. Tomić, *Adv. Phys.* **69**, 1 (2020).
 [5] K. Bender, I. Hennig, D. Schweitzer, K. Dietz, H. Endres, and H. J. Keller, *Mol. Cryst. Liq. Cryst.* **108**, 359 (1984).
 [6] Y. Takano, K. Hiraki, H. Yamamoto, T. Nakamura, and T. Taka-

- hashi, *J. Phys. Chem. Solids* **62**, 393 (2001).
- [7] T. Takahashi, Y. Nogami, and K. Yakushi, *J. Phys. Soc. Jpn.* **75**, 051008 (2006).
- [8] M. Meneghetti, R. Bozio, and C. Pecile, *Journal de Physique* **47**, 1377 (1986).
- [9] J. Moldenhauer, C. Horn, K. Pokhodnia, D. Schweitzer, I. Heinen, and H. Keller, *Synth. Met.* **60**, 31 (1993).
- [10] R. Wojciechowski, K. Yamamoto, K. Yakushi, M. Inokuchi, and A. Kawamoto, *Phys. Rev. B* **67**, 224105 (2003).
- [11] Y. Yue, K. Yamamoto, M. Uruichi, C. Nakano, K. Yakushi, S. Yamada, T. Hiejima, and A. Kawamoto, *Phys. Rev. B* **82**, 075134 (2010).
- [12] T. Ivek, B. Korin-Hamzić, O. Milat, S. Tomić, C. Clauss, N. Driehko, D. Schweitzer, and M. Dressel, *Phys. Rev. B* **83**, 165128 (2011).
- [13] K. Yakushi, *Crystals* **2**, 1291 (2012).
- [14] T. Kakiuchi, Y. Wakabayashi, H. Sawa, T. Takahashi, and T. Nakamura, *J. Phys. Soc. Jpn.* **76**, 113702 (2007).
- [15] K. Yamamoto, S. Iwai, S. Boyko, A. Kashiwazaki, F. Hiramatsu, C. Okabe, N. Nishi, and K. Yakushi, *J. Phys. Soc. Jpn.* **77**, 074709 (2008).
- [16] P. Lunkenheimer, B. Hartmann, M. Lang, J. Müller, D. Schweitzer, S. Krohns, and A. Loidl, *Phys. Rev. B* **91**, 245132 (2015).
- [17] N. Tajima, A. Ebina-Tajima, M. Tamura, Y. Nishio, and K. Kajita, *J. Phys. Soc. Jpn.* **71**, 1832 (2002).
- [18] N. Tajima, S. Sugawara, M. Tamura, R. Kato, Y. Nishio, and K. Kajita, *Eur. Phys. Lett.* **80**, 47002 (2007).
- [19] A. Kobayashi, S. Katayama, Y. Suzumura, and H. Fukuyama, *J. Phys. Soc. Jpn.* **76**, 034711 (2007).
- [20] N. Tajima, S. Sugawara, R. Kato, Y. Nishio, and K. Kajita, *Phys. Rev. Lett.* **102**, 176403 (2009).
- [21] M. Dressel, G. Grüner, J. Pouget, A. Breining, and D. Schweitzer, *Synth. Met.* **70**, 929 (1995).
- [22] K. Tamura, T. Ozawa, Y. Bando, T. Kawamoto, and T. Mori, *J. Appl. Phys.* **107**, 103716 (2010).
- [23] F. Itose, T. Kawamoto, and T. Mori, *J. Appl. Phys.* **113**, 213702 (2013).
- [24] T. Ivek, I. Kovačević, M. Pinterić, B. Korin-Hamzić, S. Tomić, T. Knoblauch, D. Schweitzer, and M. Dressel, *Phys. Rev. B* **86**, 245125 (2012).
- [25] T. Peterseim, T. Ivek, D. Schweitzer, and M. Dressel, *Phys. Rev. B* **93**, 245133 (2016).
- [26] A. Ito, Y. Nakamura, A. Nakamura, and H. Kishida, *Phys. Rev. Lett.* **111**, 197801 (2013).
- [27] K. Kodama, M. Kimata, Y. Takahide, N. Kurita, A. Harada, H. Satsukawa, T. Terashima, S. Uji, K. Yamamoto, and K. Yakushi, *J. Phys. Soc. Jpn.* **81**, 044703 (2012).
- [28] S. Uji, K. Kodama, K. Sugii, Y. Takahide, T. Terashima, N. Kurita, S. Tsuchiya, M. Kohno, M. Kimata, K. Yamamoto, and K. Yakushi, *Phys. Rev. Lett.* **110**, 196602 (2013).
- [29] T. Iimori, T. Naito, and N. Ohta, *J. Am. Chem. Soc.* **129**, 3486 (2007).
- [30] T. Iimori and N. Ohta, *J. Phys. Chem. C* **118**, 7251 (2014).
- [31] T. Ishikawa, Y. Sagae, Y. Naitoh, Y. Kawakami, H. Itoh, K. Yamamoto, K. Yakushi, H. Kishida, T. Sasaki, S. Ishihara, Y. Tanaka, K. Yonemitsu, and S. Iwai, *Nat. Commun.* **5**, 5528 (2014).
- [32] T. Osada and A. Kiswandhi, *J. Phys. Soc. Jpn.* **90**, 053704 (2021).
- [33] A. Kiswandhi and T. Osada, *J. Phys.: Condens. Matter* **34**, 105602 (2022).
- [34] R. Okazaki, Y. Nishina, Y. Yasui, F. Nakamura, T. Suzuki, and I. Terasaki, *J. Phys. Soc. Jpn.* **82**, 103702 (2013).
- [35] N. Tajima, M. Tamura, Y. Nishio, K. Kajita, and Y. Iye, *J. Phys. Soc. Jpn.* **69**, 543 (2000).
- [36] T. Gulbrandsen, N. I. Meyer, and J. Schjaer-Jakobsen, *Rev. Sci. Instrum.* **36**, 743 (1965).
- [37] M. A. Dubson, Y. C. Hui, M. B. Weissman, and J. C. Garland, *Phys. Rev. B* **39**, 6807 (1989).
- [38] C. Thibierge, D. L'Hôte, F. Ladieu, and R. Tourbot, *Rev. Sci. Instrum.* **79**, 103905 (2008).
- [39] Y. Tokura and N. Nagaosa, *Nat. Commun.* **9**, 3740 (2018).
- [40] D. G. Cahill and R. O. Pohl, *Phys. Rev. B* **35**, 4067 (1987).
- [41] I. K. Moon, Y. H. Jeong, and S. I. Kwun, *Rev. Sci. Instrum.* **67**, 29 (1996).
- [42] P. F. Sullivan and G. Seidel, *Phys. Rev.* **173**, 679 (1968).
- [43] D. H. Jung, T. W. Kwon, D. J. Bae, I. K. Moon, and Y. H. Jeong, *Meas. Sci. Technol.* **3**, 475 (1992).
- [44] G. Grüner, *Rev. Mod. Phys.* **60**, 1129 (1988); *Rev. Mod. Phys.* **66**, 1 (1994).
- [45] R. Rommel, B. Hartmann, J. Brandenburg, J. A. Schlueter, and J. Müller, *Phys. Status Solidi B* **250**, 568 (2013).
- [46] V. Moshnyaga, K. Gehrke, O. I. Lebedev, L. Sudheendra, A. Belenchuk, S. Raabe, O. Shapoval, J. Verbeeck, G. Van Tendeloo, and K. Samwer, *Phys. Rev. B* **79**, 134413 (2009).
- [47] E. J. Ryder, *Phys. Rev.* **90**, 766 (1953).
- [48] K. Behnia, *J. Phys.: Condens. Matter* **27**, 375501 (2015).
- [49] J. Wang, L. Yang, C. W. Rischau, Z. Xu, Z. Ren, T. Lorenz, J. Hemberger, X. Lin, and K. Behnia, *npj Quant. Mat.* **4**, 61 (2019).
- [50] F. Nad and P. Monceau, *J. Phys. Soc. Jpn.* **75**, 051005 (2006).
- [51] P. Lunkenheimer and A. Loidl, *J. Phys.: Condens. Mat.* **27**, 373001 (2015).
- [52] R. Martoňák and E. Tosatti, *Phys. Rev. B* **54**, 15714 (1996).
- [53] P. Morin and D. Schmitt, *Phys. Rev. B* **23**, 5936 (1981).
- [54] A. P. Ramirez, P. Coleman, P. Chandra, E. Brück, A. A. Menovsky, Z. Fisk, and E. Bucher, *Phys. Rev. Lett.* **68**, 2680 (1992).
- [55] K. Katono, T. Taniguchi, K. Ichimura, Y. Kawashima, S. Tanda, and K. Yamamoto, *Phys. Rev. B* **91**, 125110 (2015).
- [56] T. C. Umland, S. Allie, T. Kuhlmann, and P. Coppens, *J. Chem. Phys.* **92**, 6456 (1988).
- [57] S. Kitou, T. Fujii, T. Kawamoto, N. Katayama, S. Maki, E. Nishibori, K. Sugimoto, M. Takata, T. Nakamura, and H. Sawa, *Phys. Rev. Lett.* **119**, 065701 (2017).
- [58] S. Kitou, Y. Hosogi, R. Kitaura, T. Naito, T. Nakamura, and H. Sawa, *Crystals* **10**, 998 (2020).
- [59] T. Ivek, B. Korin-Hamzić, O. Milat, and S. Tomić, C. Clauss, N. Driehko, D. Schweitzer, and M. Dressel, *Phys. Rev. Lett.* **104**, 206406 (2010).
- [60] T. Ivek, M. Čulo, M. Kuveždić, E. Tutiš, M. Basletić, B. Mihaljević, E. Tafra, S. Tomić, A. Löhle, M. Dressel, D. Schweitzer, and B. Korin-Hamzić, *Phys. Rev. B* **96**, 075141 (2017).